Letter

Efficient 1.9 μm emission in H_2-filled hollow core fiber by pure stimulated vibrational Raman scattering

Zefeng Wang,[1,2] Fei Yu,[1] William J. Wadsworth,[1] and Jonathan C. Knight[1]

[1] Centre for Photonics and Photonic Materials, Department of Physics, University of Bath, Bath, BA2 7AY, UK.
[2] College of Optoelectronic Science and Engineering, National University of Defense Technology, Changsha,410073, P.R.China.

E-mail: hotrosemaths@163.com

Received xx April 2014, xx April 2014
Accepted for publication xx Month 2014
Published xx Month 2014

Abstract

We report here efficient 1.9 μm emission by pure stimulated vibrational Raman scattering in a hydrogen-filled anti-resonant hollow-core fiber pumped with a 1064 nm microchip laser. A maximum quantum conversion efficiency ~48% was achieved by using a 6.5 m length of fiber filled with 23 bar hydrogen, with a maximum peak output power of 2 kW. By properly designing the transmission bands of the fiber, selecting alternative pump sources and active gases, the emission wavelength could be extended into the mid-infrared. This provides a potential route for generating efficient, compact, broadly tunable, high power, and narrow linewidth mid-infrared fiber gas sources with broad application in defense, environmental, and medical monitoring.

Keywords: Photonic crystal fibers, fiber lasers, gas lasers, stimulated Raman scattering

1. Introduction

Since the first demonstration in 1963 [1], stimulated Raman scattering (SRS) in gases has attracted enormous attention. Because of its high Raman gain coefficient and large Raman shift, SRS in gases has been recognized as an effective method to obtain tunable, narrow linewidth light sources of otherwise unobtainable wavelengths, especially in the ultra-violet and infrared spectral range [2,3]. While, SRS in gas cells requires high pump power due to the short effective interaction length, and usually provides low conversion efficiency to the desired wavelength due to additional generation of other unwanted Raman lines.

Historically, to enhance the interaction between pump laser and Raman gases, hollow fiber capillaries [4], and high-finesse cavities [5] have been investigated. However, the interaction length remained limited, and the Stokes conversion efficiency was low (only ~5% [5]). Hollow core photonic crystal fiber (HC-PCF) [6] made it possible to obtain high conversion efficiency for SRS in gases, as it provides a near-ideal environment for SRS by combining a very long effective interaction length, high confinement of pump light in a small modal area, and the possibility of controlling the gain spectrum by wavelength-dependent fiber attenuation. Since its first demonstration in 2002 [6], there have been several reports of SRS in gas-filled HC-PCF [7-8]. High efficiency pure rotational SRS has been observed in H_2-filled HC-PCF with far lower Raman thresholds [7]. However, efficient conversion to the vibrational Stokes waves of longer wavelength has not been reported due to the limit of the current HC-PCF.

Recently, we have characterized a HC-PCF with anti-resonant core walls [9,10], which can guide light into the mid-infrared. According to the anti-resonant reflecting guidance model, if we change the core wall thickness, the high loss regions would shift, with the resonance wavelengths λ_{res} given by [9]

$$\lambda_{res} \sim \frac{2d}{m}\left(n_{clad}^2 - n_{air}^2\right)^{1/2} \quad (1)$$

where d is the thickness of the core wall, m is a positive integer, and n_{clad} and n_{air} are the refractive indexes of the cladding material and the air core respectively. According to Eq. (1), the transmission bands can be controlled, which makes it possible to exploit the large shift of vibrational SRS in hydrogen to efficiently generate longer wavelength laser emission, without the generation of other unwanted wavelengths, which is difficult for the current HC-PCF with only one single broad transmission band.

We report here the first efficient 1.9 μm wavelength convertor in anti-resonant HC-PCF filled with hydrogen by pure vibrational SRS, pumped with a linearly polarized 1064 nm microchip laser. A maximum quantum conversion efficiency ~48% is obtained with a 6.5 m fiber length and 23 bar hydrogen pressure, pumped with a linearly polarized laser. By properly designing the transmission bands, selecting alternative pump sources and active gases, this kind of hollow core fiber could offer a new method to generate efficient, compact, and tunable mid-infrared fiber gas lasers, combining the advantages of fiber and gas lasers. Compared to mid-infrared fiber lasers based on rare-earth-doped fiber [11, 12], it holds the potential to generate diffraction limited narrow-linewidth beams at high power levels which are not readily attainable with solid-core fibers. Compared to the recently demonstrated mid-infrared fiber gas source based on population inversion [13], it has the conveniences of the choosing and tuning for the emission wavelengths.

2. Experimental setup

A schematic of our experimental setup is shown in Fig. 1(a). The core diameter of the test fiber is ~53 μm. The measured attenuation spectrum (Fig. 1(b)) shows that the 1907 nm vibrational Stokes line (the $Q_{01}(1)$ Raman transition in hydrogen, Raman shift 4155 cm^{-1}) is in the first band, and the pump wavelength 1064 nm is in the second band together with the rotational Stokes line 1135 nm (the $S_{00}(1)$ Raman transition in hydrogen, Raman shift 587 cm^{-1}). The hollow core fiber is filled with high pressure hydrogen using two gas cells, and is pumped with a 1064 nm pulsed laser (linewidth ~0.25 nm, pulse duration ~0.7 ns, repetition rate 7.25 kHz, average power ~65 mW). The incident pump power is controlled using a half-wave plate and a polarization beam splitter (PBS) before being coupled into the fiber through a plano-convex lens (focal length 50 mm, AR coating 1050-1620 nm, measured transmission ~98% at 1064 nm, and ~95% at 1907 nm)

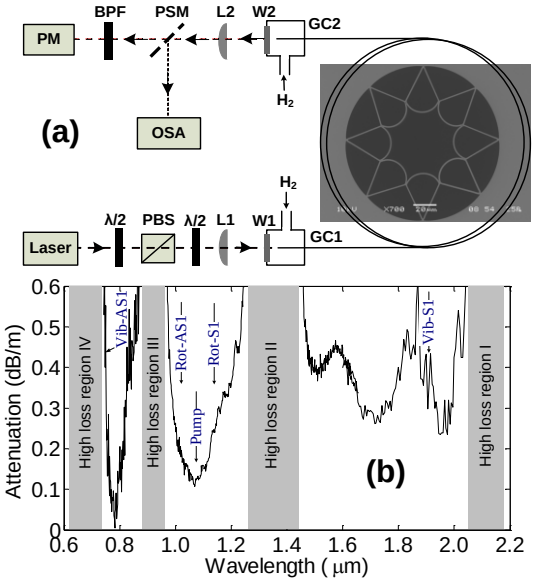

Figure 1. (a) Experimental setup: OSA, optical spectrum analyzer; PSM, silver mirror; L1,2, convex-plane lens; BPF, band pass filter; GC1,2, gas cell; PM, power meter; PBS, polarization beam splitter; λ/2, half-wave plate. *insert* the scanning electron micrograph of the test HC-PCF. (b) The measured loss of the HC-PCF, Pump: 1064 nm, 0.12 dB/m; Vib-S1: vibrational Stokes: 1907 nm, loss 0.35 dB/m; Vib-AS1: vibrational anti-Stokes, 738 nm, 0.45 dB/m; Rot-S1: rotational Stokes, 1135 nm, 0.25 dB/m; Rot-AS1: rotational anti-Stokes, 1001 nm, 0.24 dB/m.

and a silica window (W1, AR coating 1050-1620 nm, measured transmission >98% at 1064 nm). Another half-wave plate, positioned after the PBS, is used to optimize the transmitted power as the fiber is slightly polarization-dependent. The optimized fiber coupling coefficient is ~65%. The output beam passes through an uncoated silica window (W2, measured transmission ~90% at both 1064 nm and 1907 nm), and is collimated by another similar plano-convex lens (L2) before being sent to a broadband spectrometer or a power meter.

3. Experimental results and discussion

The experiments were carried out for different fiber lengths by repeated cut-back of a 29 m anti-resonant HC-PCF. For each fiber length, the vibrational SRS thresholds, transmitted power, and output spectrum were measured with different pump powers and hydrogen pressures. Here the Raman threshold is defined as the required coupled pump power causing the Stokes intensity I_s arising from spontaneous Raman scattering to an output power level that can be observed, i.e. $I_s^{th}=I_{s0}e^{G_{th}}$, where G_{th} is the thre-shold net gain factor related to measurement conditions, $I_{s0}=\Gamma/2$ is the spontaneous Stokes intensity, 2Γ is the FWHM Raman linewidth [14]. Applying this threshold condition and the Stokes intensity expression in

Ref. [14], and assuming square pulses, a universal Raman threshold expression can be obtained as

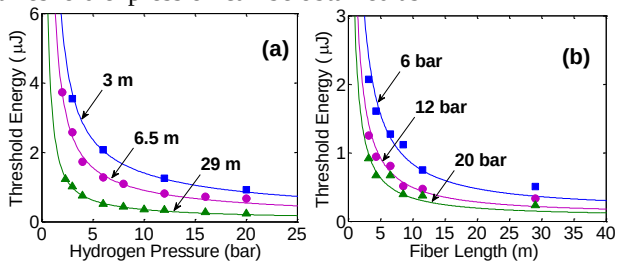

Figure 2. The evolution of vibrational SRS threshold with the hydrogen pressure and fiber length. The discrete points represent the measured data, and the solid lines are calculated from Eq. (1) for transient state with γ_g calculated from Ref. [15]: (a) G_{th}=5.4 for 3 m, 6 for 6.5 m, and 7.5 for 29 m; (b) G_{th}=6.

$$P_{th} = G'_{th}\frac{A_{eff}}{\gamma_g L_{eff}} \qquad (2)$$

where γ_g is the peak steady-state Raman gain coefficient [15]; $L_{eff}=(1-e^{-\alpha_p L})/\alpha_p$ is the effective fiber length, here α_p is the fiber attenuation at pump wavelength; A_{eff} is the effective area of the fiber modal field. In the steady state $G'_{th}=G_{th}+\alpha$, where α is a constant much smaller than G_{th}. In the transient state, $G'_{th}=[\ln(4\pi\Gamma\tau)+G_{th}]^2/(8\Gamma\tau)$, here τ is the pump pulse duration.

The Raman threshold (Fig.2) was measured using an InGaAs photo-detector (Thorlabs PDA10D, wavelength range 1.2 to 2.6 μm, bandwidth 15 MHz) to detect the Stokes pulse with a threshold condition of signal amplitude >20 mV on the oscilloscope, and the noise floor is ±5 mV. Fig. 2(a) shows that the experimental results agree well with the calculated curves, which implies that the SRS in our experiments operates at the transient state due to the sub-nanosecond pump pulses [14]. The threshold net gain factor G_{th} increases with increasing fiber length. That is due to the fiber loss at the stokes wavelength, which is not considered in the calculation. In Fig. 2(b), the differences mainly come from the fact that the calculations have been conducted with an identical G_{th}.

The measured output spectrum (Fig. 3) shows that the vibrational Stokes 1907 nm is very strong. For a 6.5 m fiber, no rotational SRS signal was observed even though the corresponding wavelengths are in the transmission bands. This is not surprising, because the vibrational SRS gain is about 2.5 times of the rotational SRS gain if the pump laser is linearly polarized [6,8]. As the transmission losses at Stokes wavelengths are much lower than the Raman gain $\gamma_g I_p$, both the spontaneous vibrational and rotational Raman scattering will linearly grow with the pump intensity at the beginning of the fiber [14]. The vibrational Raman scattering will soon become dominant due to higher Raman gain, and the intensity will then grow quasi-exponentially along the fiber length [14]. Therefore the rotational SRS will be greatly suppressed due to increasing conversion of the pump power to the vibrational Stokes signal. In addition, high pressure is beneficial for vibrational SRS, while rotational SRS is known to be most efficiently excited at lower pressure (<10 bar) [6]. With the increase of the propagation distance, the rotational Stokes waves were observed (Fig. 3 for 11 m and 29 m). We believe that this is due to the polarization degradation and non-single mode guidance of the pump beam along the fiber, and lower Raman thresholds for longer fiber length due to Eq. (2). Another interesting phenomenon is that the rotational Stokes line 770 nm, pumped by the Vib-AS1 line 737 nm, was observed for 11 m and 29 m fiber. We attribute this to the low attenuation at 770 nm (~0.07 dB/m) and the high Raman gain at 737 nm [15].

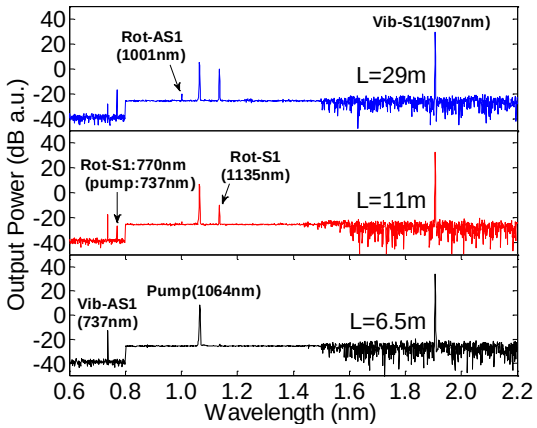

Figure 3. The transmitted optical spectrum of the 20 bar hydrogen-filled HC-PCF with 35 mW coupled pump power, the changes of the noise level at 800 nm and 1500 nm are due to change of photo-detectors inside the broadband optical spectrometer, and the relative intensities should be only taken as indicative.

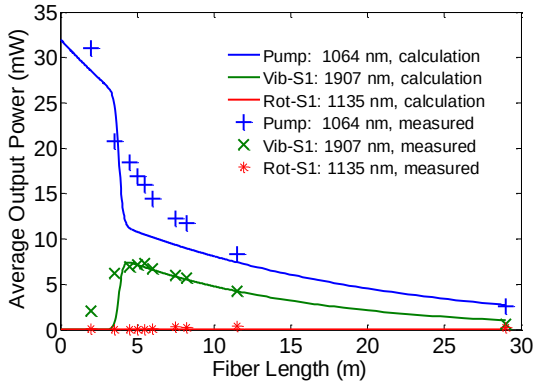

Figure 4. The evolution of output power as a function of fiber length, the hydrogen pressure is 20 bar and the coupled pump power is 32 mW for both calculations and experiments. The solid lines are calculated with: F=0.55, α_{Sv}=0.35 dB/m, α_{Sr}=0.25 dB/m, α_P=0.25 dB/m, γ_{Sv}=0.96 cm/GW calculated from Ref. [15], and γ_{Sr}=0.4 cm/GW [6,8], fiber core diameter is 53 μm, Raman FWHM linewidth is 955 MHz from Ref. [15].

Pulsed Raman processes in multi-mode hollow core fiber are very complicated, but we base our thinking on the following considerations: (1) the walk-off length for the HC-PCF is several hundred meters, which is much longer than the fiber length, so walk-off effects are negligible; (2) At high pressures, the dephasing time of hydrogen is shorter than the pump pulse duration [15], so the SRS is close to steady state (the right hand side of Fig. 2(a)); (3) Other Stokes intensities are negligible compared to the first vibrational Stokes intensity I_{Sv}, the first rotational Stokes intensity I_{Sr}, and pump intensity I_P. In this case a simple steady-state SRS model is approximately valid and can be given by [16]

$$\frac{\mathrm{d}}{\mathrm{d}z} I_{Sv} = \gamma_{Sv} I_{Sv} I_P - \alpha_{Sv} I_{Sv} \tag{3}$$

$$\frac{\mathrm{d}}{\mathrm{d}z} I_{Sr} = \gamma_{Sr} I_{Sr} I_P - \alpha_{Sr} I_{Sr} \tag{4}$$

$$\frac{\mathrm{d}}{\mathrm{d}z} I_P = -\gamma_{Sv} I_{Sv} I_P \frac{\nu_P}{\nu_{Sv}} - \gamma_{Sr} I_{Sr} I_P \frac{\nu_P}{\nu_{Sr}} - \alpha_P I_P \tag{5}$$

where z is the distance of propagation through the fiber; γ_{Sv} and γ_{Sr} are steady-state peak Raman gain coefficients for Vib-S1 and Rot-S1; α_{Sv}, α_{Sr}, and α_P are the fiber transmission attenuations at Vib-S1, Rot-S1 and pump respectively; ν_{Sv}, ν_{Sr}, and ν_P are the frequencies of Vib-S1, Rot S1 and pump respectively. In this model, a pump-Stokes modal overlap factor F is used [8], i.e. the equivalent pump intensity at the beginning of the fiber is equal to the product of the total coupled pump intensity and the overlap factor F.

The evolution of output power as a function of fiber length is shown in Fig. 4. The intensity of 1907 nm is measured with a band pass filter (Thorlabs FB2000-500, transmission ~78% at 1907 nm, $<10^{-4}$ at 1064 nm). The intensity of 1135 nm is obtained by subtracting the intensity of 1907 nm from the power after a 1064 nm long pass filter (Semrock Razor Edge, transmission >98% at both 1135 nm and 1907 nm, $< 10^{-4}$ at 1064 nm). The residual pump power is given by subtracting the power both 1907 nm and 1135 nm from the total output power. Fig. 4 shows that this simple model can roughly give the growth and decay of the pump and Stokes waves. Both the theoretical and experimental results indicate an optimum length for vibrational SRS with a given pressure and coupled pump power. The measured Vib-S1 power agrees well with the calculated values after the optimum length, which indicates that the Raman conversion has almost finished within this distance. The Stokes intensity then decreases mainly because of the transmission loss. The calculated vibrational Stokes intensity increases much more sharply than the measured results, which is due to the limitation of this steady-state model. No rotational Stokes was observed before 10 m, which agrees with the calculations. For the residual pump laser intensity, the differences between the calculations and experiments are likely to be caused by multimode pump guidance or polarization evolution in the fiber.

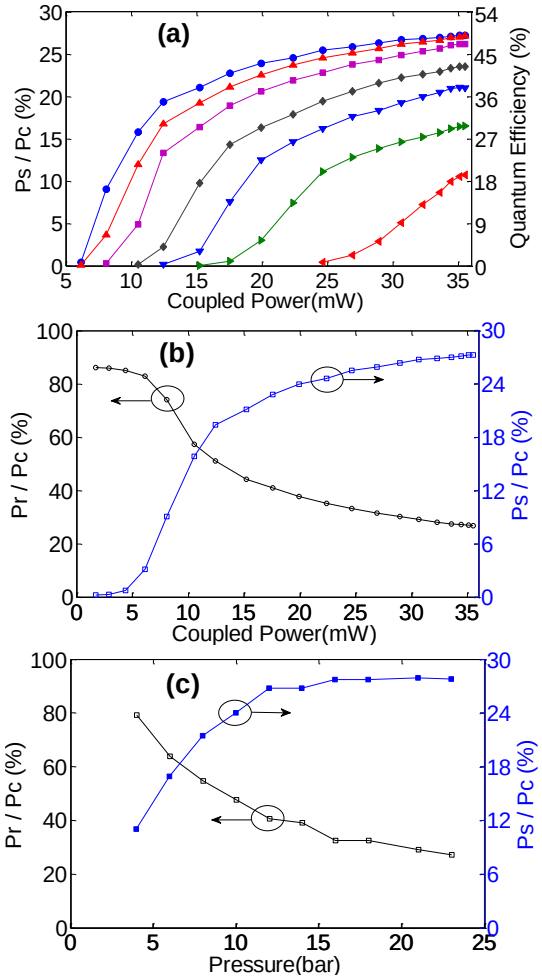

Figure 5. The output power change with the incident pump power and hydrogen pressure for 6.5 m fiber: (a) The Raman conversion efficiency is plotted versus the coupled pump power at different pressures, from top to bottom is 23, 18, 14, 10, 8, 6, and 4 bar respectively; (b) The evolution of the residual pump and the Stokes power with coupled pump power under 23 bar gas pressure; (c) The evolution of the residual pump and the Stokes power with gas pressure for 35 mW coupled pump power, here P_c, P_r, and P_s represent the coupled pump power, the residual pump power, and the stokes power respectively.

From Fig. 5, it can be seen that the output Stokes efficiency increases rapidly with increasing pump power, approaching saturation at higher pump powers. At a given input power, more Stokes is generated using higher pressures, although towards the upper end of the pump range investigated the outputs converge over the range of pressures shown. With 36 mW coupled pump power, we obtained a maximum power conversion efficiency of ~27%, corresponding to a quantum efficiency of ~48%. Output field patterns at the residual pump wavelength,

recorded by a camera, suggested multimode pump propagation, which limits the conversion efficiency and might explain the relatively strong residual pump power. The evolution of the output power versus hydrogen pressure (Fig. 5(c)) shows that the Stokes power increases sharply with increasing gas pressure below 12 bar, then approaches saturation beyond 15 bar.

4. Conclusions

In conclusion, we have demonstrated efficient single-pass 1.9 μm fiber gas Raman conversion by pure vibrational SRS in H_2-filled anti-resonant HC-PCF. The rotational SRS has been effectively suppressed by using a linearly polarized pump laser, relatively short fiber length and high hydrogen pressure, despite the spectral lines lying within the transmission bands of the hollow core fiber. A maximum quantum conversion efficiency ~48%, mainly limited by the multi-mode guidance of the fiber, was achieved by using a 6.5 m length of fiber filled with 23 bar hydrogen, and the maximum peak power reached 2000 W. We believe that this opens new opportunities for efficient, compact, tunable, high-power, and narrow-linewidth mid-infrared fiber wavelength conversion.

Acknowledgments

This work is supported by the UK Engineering and Physical Sciences Research Council (EP/I011315/1), the International Science & Technology Cooperation of China (2012DFG11470), and National Natural Science Foundation of China (11274385).

References

[1] R. W. Minck, R. W. Terhune, and W. G. Rado 1963 Laser stimulated Raman effect and resonant four-photon interactions in gases H2, D2, and CH4 *Appl. Phys. Lett.* **3** 181-183

[2] D. J. Brink, D. Proch, D. Basting, K. Hohla, and P. Lokai 1982 Efficient tunable ultraviolet source based on stimulated Raman scattering *Laser Optoelektron*. **3** 41-45

[3] T. R. Loree, C. D. Cantrell and D. L. Barker 1976 Stimulated Raman emission at 9.2 μm from hydrogen gas *Opt. Comm.* **17** 160-162

[4] P. Rabinowitz, A. Kaldor, R. Brickman, and W. Schmidt 1976 Waveguide H2 Raman laser *Appl. Opt*. **15**, 2005-2006

[5] L. S. Meng, K. S. Repasky, P. A. Roos, and J. L. Carlsten 2000 Widely tunable continuous-wave Raman laser in diatomic hydrogen pumped by an external-cavity diode laser *Opt. Lett.* **25** 472-474

[6] F. Benabid, J. C. Knight, G. Antonopoulos and P. St. J. Russell 2002 Stimulated Raman scattering in hydrogen-filled hollow-core photonic crystal fiber *Science* **298** 399-402

[7] F. Couny, F. Benabid, P. S. Light 2007 Subwatt threshold cw Raman fiber-gas laser based on H_2-filled hollow core photonic crystal fiber *Phys. Rev. Lett*. **99**, 143903-6

[8] B. M. Trabold, A. Abdolvand, T. G. Euser, A. M. Walser, and P. St.J. Russell 2013 Amplification of higher-order modes by stimulated Raman scattering in H_2-filled hollow-core photonic crystal fiber *Opt. Lett.* **38**, 600-602

[9] Fei Yu, William J. Wadsworth, and Jonathan C. Knight 2012 Low loss silica hollow core fibers for 3–4 μm spectral region *Opt. Express* **20**, 11153-11158

[10] Fei Yu and Jonathan C. Knight 2013 Spectral attenuation limits of silica hollow core negative curvature fiber *Opt. Express* **21**, 21466-21471

[11] Stuart D. Jackson 2012 Towards high-power mid-infrared emission from a fiber laser *Nature Photonics* **16**, 423-431

[12] Ori Henderson-Sapir, J. Munch, and D. J. Ottaway 2014 Mid-infrared fiber laser at and beyond 3.5 μm using dual-wavelength pumping *Opt. Lett.* **39**, 493-496

[13] A. M. Jones, A. V. V. Nampoothiri, A. Ratanavis, T. Fiedler, N. V. Wheeler, F. Couny, R. Kadel, F. Benabid, B.R. Washburn, K. L. Corwin, and W. Rudolph 2011 Mid-infrared gas filled photonic crystal fiber laser based on population inversion *Opt. Express* **19** 2309–2316

[14] M. G. Raymer, and J. Mostowski 1981 Stimulated Raman scattering: unified treatment of spontaneous initiation and spatial propagation *Physics Review A* **24**, 1980-1993

[15] W. K. Bischel and M. J. Dyer 1986 Wavelength dependence of the absolute Raman gain coefficient for Q(1) transition in hydrogen *J. Opt. Soc. Am. B* **3**, 677-682

[16] Y. R. Shen and N. Bloembergen 1965 Theory of stimulated Brillouin and Raman Scattering *Physical Review* **137**, 1787-1805